Quantitative Elastohydrodynamic Film-Forming for an Oil/Refrigerant System

Scott Bair*
Regents' Researcher
Georgia Institute of Technology, Center for High-Pressure Rheology
George W. Woodruff School of Mechanical Engineering
Atlanta, GA 30332-0405, USA
scott.bair@me.gatech.edu

Wassim Habchi[#]
Lebanese American University, Department of Industrial and Mechanical Engineering
Byblos, Lebanon
wassim.habchi@lau.edu.lb

Mark Baker and David M. Pallister
CPI Fluid Engineering, a division of The Lubrizol Corporation
2300 James Savage Road,
Midland, Michigan 48642
MRBA@CPIfluideng.com

*Corresponding Author

[#]At the time this work was done, the second author was holding a visiting scholar position at Georgia Institute of Technology

Abstract

The first calculations of film thickness for an oil/refrigerant system using quantitative elastohydrodynamics are reported in this work. It is demonstrated that primary measurements of the properties of the oil/refrigerant system can be employed to accurately predict film thickness in concentrated contacts. An unusual response to lubricant inlet temperature is revealed wherein the film thickness may increase with temperature as a result of decreasing refrigerant solubility in oil when the inlet pressure is high. There is competition between the reduction in viscosity of

the oil and the reduction of refrigerant concentration with increased temperature. For high inlet pressure, the dilution effect is dominant, whereas for low inlet pressure, the temperature dependence of the viscosity of the solution dominates over the range of inlet temperatures considered.

KEYWORDS: elastohydrodynamic, film thickness, pressure-viscosity, compressibility, oil/refrigerant lubrication

1. INTRODUCTION

An alternative to the classical approach to understanding film-forming in elastohydrodynamic lubrication (EHL) has appeared in the last ten years or so. Previously, in EHL analyses, the properties of the liquid were adjusted to provide agreement between experiment and theory using models based upon fictional accounts of viscosity measurements. The first Newtonian EHL calculation of film thickness employing primary measurements of viscosity and compressibility did not appear until 2006 [1] and was shortly followed by the first full simulation of film thickness and friction from real shear-thinning [2]. Although the classical approach persists in places, there has since been a revolution in understanding the EHL problem [3-11] through the use of primary measurements in EHL analysis, that is, quantitative elastohydrodynamics.

In this work, the quantitative EHL film thickness analysis is extended to the very challenging problem of calculating film thickness for a concentrated contact lubricated by oil diluted with refrigerant. Within the environment of a refrigeration compressor, the lubricating oil is in contact with refrigerant vapor with which it is miscible. The film which protects the contact from wear must therefore be generated from oil which has had the viscosity reduced by the dissolved refrigerant. The viscosity reduction can be sufficient to result in increasing bearing wear and failure [12, 13].

The viscosity of the oil/refrigerant system (oil/refrigerant system is the term used by CPI) is usually known at saturation conditions; however, the effect of pressure on the system is also required for the determination of EHL film thickness. The approach most often taken has been to invoke the concept of a pressure-viscosity coefficient which may be used in a classical film thickness formula to calculate the film thickness. A pressure-viscosity coefficient is a parameter that is intended to quantify the piezoviscous response of lubricants at the low pressures characteristic of the EHL inlet zone. Along with the ambient pressure viscosity, μ_0, the pressure-viscosity coefficient may be used to determine central and minimum film thicknesses from empirical formulae. There have been many definitions of the pressure-viscosity coefficient; at least six can be identified [14], making the choice of coefficient and the appropriate formula confusing even if pressure-viscosity data are available. For oil/refrigerant systems the

measurement of viscosity at elevated pressure is not straightforward as it is for the neat oil which, in contrast to the refrigerant, may be added to the viscometer at ambient pressure.

There are several reported viscosity measurements of oil/refrigerant systems at saturation pressure, for example [15]. Some have succeeded in measuring the viscosity at pressures above saturation. Comuñas et al. [16] measured the viscosity of an oil/refrigerant system to 140 MPa, however, the mass fractions of oil were less than those occurring in a compressor bearing. Jonsson and Lilje [17] employed reasonable concentrations but only reached 34 MPa. For most definitions of pressure-viscosity coefficient, the viscosity must increase by at least twenty times for a reasonable determination and this requires much greater pressure.

The alternative approach has been to measure central film thickness in a pressurized EHL optical simulator. The pressure-viscosity coefficient is then adjusted to provide agreement with a classical film thickness formula. This procedure has been shown to be highly inaccurate for even neat oils [18].

Vergne and coworkers [19] have applied the quantitative elastohydrodynamic method to the EHL film-forming with a neat refrigerant lubricant. In the current article, the EHL film thickness for a contact similar to one in a refrigeration compressor bearing is calculated for the first time from primary measurements of the pressure dependence of viscosity [20] and density [21] for an oil/refrigerant system. The film-forming capability of such systems under various inlet conditions and operating loads and speeds is investigated.

2. PROPERTY RELATIONS

The oil/refrigerant system selected for this work corresponds to a blend of polyolester oil, RL68H, and a hydro-fluoro-carbon (HFC) refrigerant, R134a. This selection has been preferred for two reasons: first, such a combination is commonly used in compressors for refrigeration systems and second, the rheological properties of this system (or at least its components) have been well characterized in [21] and [22]. A wide variety of alternative combinations may be found for refrigeration systems. However, the analysis of all possible combinations is beyond the scope of the current work. The general idea of this work is to simply provide a framework with

which quantitative film thickness prediction in oil/refrigerant lubricated contacts is made possible. Nonetheless, many of the findings reported later could be generalized to different types and combinations of oil/refrigerant mixtures. The viscosity and density of the RL68H oil, with varying mass fraction of R134a refrigerant will be represented by relationships fitted to measurements made at elevated pressures.

2.1 **Equation of State**

It is expected that a simple equation of state (EoS), relating the density or volume to temperature, pressure and mass fraction of refrigerant will be difficult to find. In EHL, the compressibility is second order to viscosity unless a viscosity correlation requires the EoS. Therefore less importance is placed on the accuracy of the EoS. The relative volumes of both RL68H and the system, 9.2% by weight of R143a in RL68H, have been measured with a metal bellows piezometer in reference [21] at 20 and 50°C to 300 MPa. The density of R134a as a function of temperature and pressure to 400 MPa was extrapolated from a correlation in reference [22]. The Tait EoS is written for relative volume or reciprocal relative density as

$$\frac{V}{V_R}=\frac{\rho_R}{\rho}=\left[1+a_V\left(T-T_R\right)\right]\left\{1-\frac{1}{1+K_0'}\ln\left[1+\frac{p}{K_0}\left(1+K_0'\right)\right]\right\} \qquad (1)$$
$$K_0=K_{00}\exp\left(-\beta_K T\right)$$

The relative volume of the liquid is V/V_R where the reference volume is $V_R=V\left(T_R=20^{\circ}\text{C},\ p=0.1\ \text{MPa}\right)$. For the neat oil, $\rho_R=977$ kg/m^3, although this value is not required for a calculation of film thickness.

From the relative volume data for both the neat oil and the oil plus refrigerant at 20 and 50°C and from the refrigerant densities at 50°C it was found that a reasonable correlation could be derived from equation (1) with K'_0 and a_v fixed at the values for the neat oil. The correlation then requires that K_{00} vary with refrigerant concentration by weight, c_1, as

$$K_{00}=K_{oil}\left(1-c_1\right)^{Q_K}+K_{refr} \qquad (2)$$

and that β_K obey

$$\beta_K=\beta_{Koil}\left(1-c_1\right)^{Q_\beta}+\beta_{Krefr} \qquad (3)$$

The parameters for equations (2) and (3) are given in Table 1 and the validation of the EoS (1-3) is shown in Figure 1 for 50°C. The volumes are plotted relative to a pressure of 10MPa. The excellent agreement for the neat refrigerant at 50°C should not be representative of other temperatures because the thermal expansivity of the refrigerant is not well-represented by the value of a_v employed here; however, neat refrigerant is not the central topic.

2.2 **Viscosity Correlation with Temperature, Pressure and Concentration**

The low shear viscosity of the oil was measured at 30, 60 and 100°C to 350 MPa using the technique of reference [20]. The low shear viscosity was measured at refrigerant mass concentrations of c_1=0.154 and 0.228 using the same technique. Viscosities are listed in Table 2.

2.2.1 Correlation of Oil Viscosity

The improved Yasutomi [23] correlation is

$$\mu = \mu_g \exp\left[\frac{-2.303C_1\left(T-T_g\right)F}{C_2+\left(T-T_g\right)F}\right] \quad (4)$$

where T_g is the glass transition temperature which varies with pressure as $T_g = T_{g0} + A_1 \ln\left(1+A_2 p\right)$. The dimensionless relative thermal expansivity of the free volume, is $F = \left(1+b_1 p\right)^{b_2}$. The glass viscosity, μ_g, was assumed to have the universal value of 10^{12} Pa·s. The parameters for the oil, RL68H, are listed in Table 3.

2.2.2 Correlation of Refrigerant Viscosity

The refrigerant viscosity was modeled at 40, 75 and 100°C for pressures from 10 to 400 MPa using data from reference [22]. The refrigerant is operating far from the glass transition and may not be a glass-former. Therefore, the McEwen model [24], which is widely considered as the most accurate relation for low viscosity liquids far from the glass point, was used.

$$\mu = \mu_0 \left(1 + \frac{\alpha_0}{q} p \right)^q \qquad (5)$$

Here $\alpha_0 = \partial \ln \mu / \partial p$ at $p = 0$. Of course, this definition is no longer sensible because the material would be a gas for pressure approaching zero. The McEwen equation may be modified for temperature by making α_0, μ_0 and q functions of temperature. The Andrade equation [25] has been applied to $\mu_0(T)$.

$$\mu_0 = \mu_\infty \exp\left[\frac{E_a}{R_g T} \right] \qquad (6)$$

Here, R_g is the gas constant and E_a is the activation energy for flow. In addition $\alpha_0 = a_0 + a_1/T$ and $q = d_0 + d_1/T$. The parameters are listed in Table 4. In regressing these parameters, the viscosity at 10 MPa and 100°C was excluded. The influence of the proximity to the vapor dome can severely decrease the viscosity at low pressure and high temperature in a way which cannot be captured by this simple correlation.

2.2.3 Viscosity Mixing Rule

The Grunberg-Nissan mixing law [26] is for concentration expressed in mole fractions, x_i, where *i*=1 for the refrigerant and *i*=2 for the oil.

$$\mu = \exp\left(x_1 \ln \mu_1 + x_2 \ln \mu_2 + x_1 x_2 g \right), \quad x_2 = 1 - x_1 \qquad (7)$$

If M_1 is the molecular mass of the refrigerant and M_2 that of the oil:

$$x_1 = \frac{1}{\left[1 + \frac{M_1}{M_2} \left(\frac{1}{c_1} - 1 \right) \right]} \qquad (8)$$

The molecular mass ratio, M_1/M_2 is treated as an unknown and is not the true molecular mass ratio. The Grunberg-Nissan mixing law is generally not accurate for oil/refrigerant systems

without this modification; M_2 must be less than the oil molecular mass. The parameters are listed in Table 5 and the predicted viscosities are compared with some of the measured viscosities in Figure 2. Obviously, the viscosity of the mixture decreases with increased refrigerant concentration because the refrigerant viscosity is orders of magnitude lower than that of the oil. The refrigerant concentration in the oil increases with pressure but decreases with temperature as discussed next.

2.3 **Refrigerant Concentration at Sump Temperature and Pressure**

A Daniel plot was supplied by the oil manufacturer from which the following empirical equation was obtained for temperatures above 50°C.

$$c_1 = \left[\frac{T_{in}}{B p_{in}^{\ E}} \right]^{1/D} \qquad (9)$$

Subscript "in" indicates the EHL inlet condition for the oil and is assumed to be the absolute temperature, T_{in}, and pressure, p_{in}, of the compressor sump or reservoir. The parameters are found in Table 6. The negative value for the parameter D implies that the refrigerant concentration within the oil increases with sump pressure but decreases with sump temperature. This makes the temperature-viscosity dependence of the oil/refrigerant mixture rather complex compared to that of the neat oil or refrigerant. In fact, for pure substances, viscosity typically decreases with increased temperature. For the oil/refrigerant mixture, increased temperature involves two competing effects: a decreased viscosity for both components which tends to decrease the overall viscosity of the mixture but also a reduced refrigerant concentration which tends to increase viscosity. This induces a rather unusual effect on film thickness for oil/refrigerant systems as will be discussed later.

3. FILM CALCULATIONS

3.1 **The Finite Element Full-System Approach**

Film thickness calculations are carried out using the finite element full-system approach developed by Habchi et al. [27]. The approach is based on a simultaneous finite element resolution of the different EHL equations: the Reynolds equation governing the hydrodynamic pressure generation within the lubricant film, the linear elasticity equations governing the elastic deformation of the contacting solids and the load balance equation which balances the pressure generated within the lubricating film with the external applied load. Smooth circular contacts subject to a constant external applied load F are considered. The geometry of such contacts can be reduced to an equivalent simplified one corresponding to a contact between a ball of radius R and a flat plane. Contacting surfaces are assumed to have constant speeds in the mean entrainment direction and film thicknesses are evaluated under pure-rolling conditions. Given the relatively low viscosity of the oil/refrigerant mixture considered in this work and the pure-rolling condition, the Newtonian limit is unlikely to be exceeded. Also, for the same reasons, no significant heat generation is expected to occur within the lubricant film. Therefore, isothermal Newtonian conditions are assumed. Given that, in the current work, a pressurized lubricant reservoir with an inlet pressure p_{in} greater than atmospheric pressure is considered, the usual zero pressure boundary conditions for Reynolds equation, at the inlet and outlet of the contact, imply in this case that the computed pressure distribution corresponds to the pressure rise above the ambient level ($p = p_{in}$). That is, in the current case, the zero pressure level in the simulations corresponds to p_{in} rather than atmospheric pressure, as is the case in standard EHL simulations. Also, on the contact outlet side, p_{in} is considered to be the vapor pressure of the oil/refrigerant mixture at the contact outlet, rather than atmospheric pressure, as is the case in standard EHL simulations. This being said, in the employed equations of state and the viscosity-p-T relations, the employed pressure is $p+p_{in}$, where p is the pressure distribution resulting from the simulations. For more details about the numerical technique (geometry, meshing, element types, finite element formulations, etc.), the reader is referred to [27].

3.2 **Experimental Validation**

First, the analysis technique was validated with the film thickness measurements of Gunsel and Pozebanchuk [28] who employed the same oil/refrigerant system, RL68H plus R134a, in interferometric determinations of the central film thickness in a circular glass/steel

contact. The load, F=20N, resulted in maximum contact pressure of 0.55 GPa from a 19.05 mm diameter steel ball against a glass disc. The inlet condition that is simulated here is T_{in} =65°C and p_{in} =1.171 MPa. The rolling velocity was varied from 0.1 to 10 m/s in the simulation and the results are plotted in Figure 3. The agreement is excellent, providing a proper validation of the proposed methodology. It must be emphasized that no liquid property was adjusted to obtain this result; only primary rheological measurements were used.

3.3 **Results**

The central film thickness, h_c , and minimum film thickness, $h_{\min}$, were calculated for the case of a steel-on-steel circular contact with an equivalent ball radius R=9.5 mm. The rolling velocity was varied from 0.1 to 10 m/s and the Hertz pressure was 0.7 and 1.0 GPa. Calculations were performed for inlet pressures of 0.5, 1 and 2 MPa and for inlet temperatures of 50, 70 and 90°C. The results are listed in Table 7. Note that sub-nanometer results were removed from Table 7 for their lack of physical relevance as well as the questionable validity of continuum mechanics and the Reynolds equation and assumptions under such extreme conditions. These extremely thin films arise at the lowest mean entrainment speeds and highest inlet pressure considered in this work. Also, any reported film thicknesses below 5 nm are to be taken with caution. In fact, even though perfectly smooth surfaces are assumed in this work, it is to be kept in mind that the notion of a perfectly smooth surface is a hypothetical / theoretical one. In practice, even the best finished surfaces have a root-mean-square (rms) surface roughness of the order of a few nanometers. As such, metal-to-metal contact is likely to occur when film thicknesses are of a few nanometers and a full EHL film is not guaranteed. A mixed lubrication regime would be more appropriate to analyze such contacts.

Increasing the inlet pressure is always seen to reduce the film thickness because of the increased solubility of the refrigerant in oil which reduces the overall viscosity of the mixture. There are, however, competing effects of temperature. Increasing the inlet temperature decreases the viscosity of the neat oil and that of the refrigerant but also decreases the solubility and therefore the refrigerant concentration. This latter effect may increase the overall viscosity of the oil/refrigerant mixture as stated earlier. The result is that increasing inlet temperature can either increase or decrease film thickness.

Further calculations were done to examine this effect. See Figures 4 and 5 where central and minimum film thicknesses, respectively, are plotted versus inlet temperature for three inlet pressures at Hertz pressure of 0.7 GPa. For p_{in} =0.5 MPa, thickness always decreases with temperature; whereas for 2 MPa it always increases with temperature. In fact, at the lowest considered inlet pressure of 0.5 MPa, the refrigerant concentration within the oil is relatively low (c_1=12.76% at T_{in}=50^{o}C). As such, any temperature increase would only lead to a relatively low variation in refrigerant concentration (c_1=7.99% at T_{in}=70^{o}C and c_1=5.14% at T_{in}=90^{o}C). Therefore, the temperature-viscosity dependence of the oil and refrigerant remains the dominant effect and leads to a continuous decrease in film thickness with inlet temperature. On the other hand, at the highest considered inlet pressure of 2 MPa, the refrigerant concentration within the oil is relatively high (c_1=62.44% at T_{in}=50^{o}C). As such, any temperature increase would lead to significant variations in refrigerant concentration (c_1=39.11% at T_{in}=70^{o}C and c_1=25.16% at T_{in}=90^{o}C). In this case, the refrigerant concentration decrease with inlet temperature is the dominant effect and film thicknesses continuously increase with inlet temperature. For p_{in} =1 MPa, the film thicknesses have a maximum value at temperatures between 70 and 75°C. At this intermediate inlet pressure, refrigerant concentrations within the oil are not sufficiently high for the refrigerant concentration effect to dominate film thickness variations with inlet temperature and are not too low for the temperature-viscosity dependence of the mixture to take-over (c_1=28.22% at T_{in}=50^{o}C, c_1=17.68% at T_{in}=70^{o}C and c_1=11.37% at T_{in}=90^{o}C). As such, at low inlet temperatures (less than 70 to 75^{o}C), refrigerant concentration effect is the dominant one and film thicknesses increase with inlet temperature. However, at higher temperatures, it is the viscosity decrease of the mixture that governs and film thicknesses decrease with inlet temperature.

To investigate farther, the viscosity at 100 MPa is plotted versus inlet temperature in Figure 6 for the three inlet pressures. This pressure may be considered representative of the contact inlet zone pressure sweep. The same trend can be seen for this viscosity as for the film thicknesses. For p_{in} =0.5 MPa, viscosity at 100 MPa always decreases with temperature; whereas for 2 MPa it always increases with temperature. For p_{in} =1 MPa, the viscosity has a maximum value at temperatures between 70 and 75°C. This is not surprising though, since inlet lubricant viscosity is known to be a governing parameter for film-forming capability in EHL

contacts. As such, it is the viscosity variation with temperature of the oil/refrigerant system that is responsible for this rather unusual film thickness behavior. Typically, for neat oils, film thicknesses tend to simply decrease with increasing inlet temperatures.

The compressibility of the liquid also influences the film thickness, although of less importance than viscosity. The volume at p=0.7 GPa relative to the volume at ambient pressure is plotted in Figure 7 as a function of inlet temperature for the three considered inlet pressures. For p_{in} =1 and 2 MPa, the relative volume at p=0.7 GPa is steadily increasing with inlet temperature. There are also two competing effects at work. Liquids naturally become more compressible with increasing temperature; however, the temperature increase reduces the concentration of the more compressible component, the refrigerant.

The effect of compressibility on film thickness is very small in comparison to viscosity as the central thickness tends to vary in proportion to the compressed volume [29, 30]. Therefore the 19% increase in compressed volume going from 50 to 90°C at p_{in} =2 MPa will only change the film thickness by 19%. Note that an increase in relative volume implies an increase in film thickness while a decrease in relative volume reduces film thickness. Therefore, at the highest considered inlet pressure of 2 MPa, the continuous increase in relative volume with inlet temperatures assists in the film thickness increase reported earlier. The same can be said at the intermediate pressure of 1MPa up to an inlet temperature of 70 to 75^{o}C. At higher inlet temperatures, the relative volume increase still tends to increase film thickness, however, the slower increase in relative volume with inlet temperature makes this effect rather weak. As such, it is governed by the temperature-viscosity dependence of the mixture, as discussed earlier, which leads to decreasing film thicknesses with increased inlet temperature. Finally, at the lowest considered inlet pressure of 0.5 MPa, relative volume variations are rather too small to induce any significant effect on film thickness. Under these conditions, the film-forming capability of the contact is governed by the viscosity decrease of the mixture with inlet temperature, leading to the continuous decrease in film thickness with inlet temperature reported earlier.

An interesting observation can be made regarding the ratio of minimum to central film thickness. The minimum film thickness is widely regarded as the most important practical

parameter of EHL in regard to wear of machine elements. For the calculations reported in Table 7, the ratio, $h_c/h_{\min}$, may be as high as 3, being greatest for the thinner films.

4. CONCLUSIONS

It was demonstrated in this work that primary measurements of the properties of the oil/refrigerant system can be employed to very accurately calculate film thickness for concentrated contacts in refrigerant compressors. Important parameters are the temperature and pressure of the liquid at the inlet to the contact which may be taken to be the temperature and pressure of the oil reservoir. A unique aspect of the problem is the two-component system of oil and refrigerant, the oil having typically one thousand times greater viscosity than the refrigerant which dilutes it. Inlet temperature and pressure determine the concentration of refrigerant and, therefore, the viscosity and compressibility of the mixture. Increasing the inlet pressure always reduces film thickness because of the increased solubility of the refrigerant in oil. Temperature, however, may cause an increase or decrease in film thickness depending on the inlet pressure. In fact, it was found that inlet temperature presents two competing effects. On one hand, increasing temperature reduces the viscosity of the components, tending to reduce overall viscosity. But on the other hand, for increasing temperature the concentration of the lower viscosity component, the refrigerant, is reduced, tending to an increase in the overall viscosity of the mixture. The first effect was found to be dominant at the lowest inlet pressure considered in this work while the second took over at the highest considered inlet pressure, over the entire range of considered inlet temperatures. At intermediate inlet pressure, the second effect was found to be dominant up to a certain threshold inlet temperature, beyond which the first effect took over. When the first effect was found to dominate film-forming capability, film thicknesses behaved normally, exhibiting a decrease with increased inlet temperatures. However, when the second effect took over, film thicknesses behaved in a rather unusual way exhibiting an increase with increased inlet temperatures. Compressibility was also found to have an effect, but secondary to viscosity.

NOMENCLATURE

a_0, a_1, d_0, d_1	parameters of the temperature modified McEwen equation (various units)
$A_1, A_2, b_1, b_2, C_1, C_2$	Yasutomi parameters (various units)
a_V	thermal expansivity defined for volume linear with temperature, K^{-1}
E_a	activation energy (J/kmol)
E, D	exponents in the saturation concentration relation
F	contact external applied load, N
g	interaction parameter in the Grunberg-Nissan mixing law
h_c	central film thickness, m
$h_{\min}$	minimum film thickness, m
K_0	isothermal bulk modulus at $p = 0$, Pa
K_0'	pressure rate of change of isothermal bulk modulus at $p = 0$
K_{00}	K_0 at zero absolute temperature, Pa
p	pressure, Pa
p_{in}	inlet or reservoir pressure, Pa
Q	exponent in the equation of state
q	exponent in the McEwen equation
R	ball equivalent radius, m
R_g	universal gas constant (8314 J/kmol·K)
T	temperature, K
T_R	reference temperature, K
V	specific volume at T and p, m^3/kg
V_R	specific volume at reference state, T_R, $p = 0$, m^3/kg
α_0	conventional or initial pressure-viscosity coefficient, Pa^{-1}
β_K	temperature coefficient of K_0, K^{-1}

μ	limiting low-shear viscosity, $\mathrm{Pa \cdot s}$
μ_R	low-shear viscosity at reference state, T_R, $p = 0$, $\mathrm{Pa \cdot s}$
μ_∞	low-shear viscosity for zero argument of the exponential, $\mathrm{Pa \cdot s}$
ρ	mass density, $\mathrm{kg/m^3}$
ρ_R	mass density at reference state, T_R, $p = 0$, $\mathrm{kg/m^3}$

REFERENCES

1. Liu, Y., Wang, Q. J., Wang, W., Hu, Y., Zhu, D., Krupka, I., & Hartl, M. (2006). EHL simulation using the free-volume viscosity model. *Tribology Letters*, *23*(1), 27-37.

2. Liu, Y., Wang, Q. J., Bair, S., & Vergne, P. (2007). A quantitative solution for the full shear-thinning EHL point contact problem including traction. *Tribology Letters*, *28*(2), 171-181.

3. Liu, Y., Wang, Q. J., Krupka, I., Hartl, M., & Bair, S. (2008). The shear-thinning elastohydrodynamic film thickness of a two-component mixture. *Journal of tribology*, *130*(2), 021502.

4. Krupka, I., Bair, S., Kumar, P., Khonsari, M. M., & Hartl, M. (2009). An experimental validation of the recently discovered scale effect in generalized Newtonian EHL. *Tribology letters*, *33*(2), 127-135.

5. Krupka, I., Kumar, P., Bair, S., Khonsari, M. M., & Hartl, M. (2010). The effect of load (pressure) for quantitative EHL film thickness. *Tribology letters*, *37*(3), 613-622.

6. Habchi, W., Bair, S., Qureshi, F., & Covitch, M. (2013). A Film Thickness Correction Formula for Double-Newtonian Shear-Thinning in Rolling EHL Circular Contacts. *Tribology Letters*, *50*(1), 59-66.

7. Habchi, W., Vergne, P., Bair, S., Andersson, O., Eyheramendy, D., & Morales-Espejel, G. E. (2010). Influence of pressure and temperature dependence of thermal properties of a lubricant on the behaviour of circular TEHD contacts. *Tribology International*, *43*(10), 1842-1850.

8. Habchi, W., Bair, S., & Vergne, P. (2013). On friction regimes in quantitative elastohydrodynamics. *Tribology International*, *58*, 107-117.

9. Björling, M., Habchi, W., Bair, S., Larsson, R., & Marklund, P. (2013). Towards the true prediction of ehl friction. *Tribology International*, *66*, 19-26.

10. Björling, M., Habchi, W., Bair, S., Larsson, R., & Marklund, P. (2014). Friction Reduction in Elastohydrodynamic Contacts by Thin-Layer Thermal Insulation. *Tribology Letters*, *53*(2), 477-486.

11. Bair, S., Habchi, W., Sperka, P., & Hartl, M. (2016). Quantitative elastohydrodynamic film forming for a gear oil with complex shear-thinning. *Proceedings of the Institution of Mechanical Engineers, Part J: Journal of Engineering Tribology*, *230*(3), 289-299.

12. Tuomas, R., & Isaksson, O. (2009). Measurement of lubrication conditions in a rolling element bearing in a refrigerant environment. *Industrial Lubrication and Tribology*, *61*(2), 91-99.

13. Jonsson, U. J., & Hansson, N. (1998). Lubrication limits of rolling element bearings in refrigeration compressors. *International Compressor Engineering Conference.* Paper 1228. http://docs.lib.purdue.edu/icec/1228

14. Bair, S. (2000). Pressure-viscosity behavior of lubricants to 1.4 GPa and its relation to EHD traction. *Tribology Transactions*, *43*(1), 91-99.

15. Geller, V. Z., Paulaitis, M. E., Bivens, D. B., & Yokozeki, A. (1996). Viscosities of HFC-32 and HFC-32/lubricant mixtures. *International journal of thermophysics*, *17*(1), 75-83.

16. Comuñas, M. J., Baylaucq, A., Boned, C., & Fernandez, J. (2004). Dynamic viscosity for HFC-134a+ polyether mixtures up to 373.15 K and 140 MPa at low polyether concentration. Measurements and modeling. *Industrial & engineering chemistry research*, *43*(3), 804-814.

17. Jonsson, U. J., & Lilje, K. C. (1998). Elastohydrodynamic Lubrication Properties of Polyol Ester Lubricants-R134a Mixtures. International Compressor Engineering Conference. Paper 1227.http://docs.lib.purdue.edu/icec/1227 34MPa

18. Bair, S. (2015). A critical evaluation of film thickness-derived pressure–viscosity coefficients. *Lubrication Science*. 27(6), pp. 337–346.

19. Vergne, P., Fillot, N., Bouscharain, N., Devaux, N., & Morales-Espejel, G. E. (2015). An experimental and modeling assessment of the HCFC-R123 refrigerant capabilities for lubricating rolling EHD circular contacts. *Proceedings of the Institution of Mechanical Engineers, Part J: Journal of Engineering Tribology*, *229*(8), 950-961.

20. Bair, S. (2016). A New High-Pressure Viscometer for Oil/Refrigerant Solutions and Preliminary Results. *Tribology Transactions,* (just-accepted), 1-32.

21. Bair, S., Baker, M., & Pallister, D. M. (2016). Revisiting the Compressibility of Oil/Refrigerant Lubricants. *Journal of Tribology*. doi:10.1115/1.4033335

22. Laesecke, A., & Bair, S. (2011). High-pressure viscosity measurements of 1, 1, 1, 2-tetrafluoroethane. *International Journal of Thermophysics*, *32*(5), 925-941.

23. Bair, S., Mary, C., Bouscharain, N., & Vergne, P. (2013). An improved Yasutomi correlation for viscosity at high pressure. *Proceedings of the Institution of Mechanical Engineers, Part J: Journal of Engineering Tribology*, 227(9), pp. 1056-1070.

24. McEwen, E. (1952). The Effect of Variation of Viscosity with Pressure on the Load-Carrying Capacity of the Oil Film between Gear-Teeth. *J. Inst. Pet*, *38*(344-345), 646-672.

25. Andrade, E. D. C. (1930). The Viscosity of Liquids. *Nature*, *125*, 309-310.

26. Grunberg, L., & Nissan, A. H. (1949). Mixture law for viscosity. *Nature*, *164*, 799-800.

27. Habchi W., Eyheramendy D., Vergne P. and Morales-Espejel G. E. – Stabilized Fully-Coupled Finite Elements for Elastohydrodynamic Lubrication Problems, *Advances in Engineering Software*, 2012, vol. 46, pp. 4-18.

28. Gunsel, S., & Pozebanchuk, M. (1999). *Elastohydrodynamic Lubrication with Polyolester Lubricants and HFC Refrigerants, Final Report, Volume 1* (No. DOE/CE/23810-102-Vol. 1). Air Conditioning and Refrigeration Technology Institute, Arlington, VA (US).

29. Venner, C. H., Bos, J.: Effects of Lubricant Compressibility on the Film Thickness in EHL Line and Circular Contacts. *Wear* 173, 151-165 (1994).

30. Habchi W. and Bair S. : Quantitative Compressibility Effects in Thermal Elastohydrodynamic Circular Contacts, *ASME Journal of Tribology*, 2013, vol. 135 (1), 011502.

Table 1. Equation of State parameters.

K'_0	10.232
a_v	7.323×10^{-4} K^{-1}
K_{oil}	9.162 GPa
Q_K	9.627
β_{Koil}	0.005723 K^{-1}
Q_β	6.815
K_{refr}	0.126 GPa
β_{Krefr}	5.8×10^{-4} K^{-1}

Table 2. Solution viscosities in mPa·s for RL68H plus weight % R134a

	0%			15.4%			22.8%		
p/MPa	30°C	60°C	100°C	30°C	60°C	100°C	30°C	60°C	100°C
0.1	113.8	29.7	8.82						
10				24.5	8.94	3.68	13.8	5.99	2.86
25	205	47.56	13.8	32.1	11.4	4.87	18.2	7.80	3.47
50	352	74.0	20.3	50.1	16.9	6.75	27.3	11.1	4.70
100	926	164	39.3	111.9	33.3	12.0	57.3	21.0	8.46
150	2406	350	69.3	242	62.9	20.1	115	37.5	13.3
250	16410	1362	207	996	198	51.0	410	107	32.0
350	110900	5084	612						
400					971	193	2486	443	99.1

Table 3. Yasutomi parameters for the oil.

Material	RL68H
T_{g0} / °C	-82.15
A_1 / °C	1467.2
A_2 / GPa^{-1}	0.0740
b_1 / GPa^{-1}	9.44
b_2	-0.3377
C_1	16.24
C_2 / °C	28.55

Table 4. Parameters for the viscosity of the refrigerant.

Material	R134a
μ_∞ / mPa·s	0.010796
E_a / J/kmol	7.47×10^6
a_0 / GPa^{-1}	12.29
a_1 / K·GPa^{-1}	-21.29
d_0	0.9673
d_1 /K	110.11

Table 5. Parameters for the Grunberg-Nissan mixing law

Material	RL68H +R134a
g	1.51
$\frac{M_1}{M_2}$	0.444

Table 6. Parameters for relating concentration to temperature and pressure

Material	RL68H +R134a
E	0.1471
B	274.7 K·MPa^{-E}
D	-0.1284

Table 7. Calculated film thickness in nm.

	Hertz Pressure/GPa=	0.7						1.0					
	T_{in} / °C=	50		70		90		50		70		90	
p_{in} / MPa	Speed /m/s	h_c / nm	h_{min} / nm	h_c / nm	h_{min} / nm	h_c / nm	h_{min} / nm	h_c / nm	h_{min} / nm	h_c / nm	h_{min} / nm	h_c / nm	h_{min} / nm
0.5	0.1	23.4	9.33	19.0	7.36	14.4	5.48	20.4	6.50	16.5	4.95	12.43	3.53
	0.2	37.9	17.2	30.8	13.4	23.4	9.65	33.3	12.3	27.0	9.56	20.4	6.72
	0.4	61.1	30.5	49.7	23.9	37.8	17.5	54.4	21.9	44.1	16.9	33.2	12.6
	1	114.3	64.8	93.1	50.8	70.7	37.2	104	49.1	83.9	38	63.3	27.2
	2	182	113	149	88.9	113	65.2	168	88.3	136	68.5	103	49.5
	4	289	195	236	154	180	113	270	157	219	122	166	88.2
	10	521	388	428	309	329	230	501	330	408	258	309	187
1.0	0.1	9.27	3.38	11.1	4.14	10.62	3.91	7.84	1.91	9.48	2.48	9.07	2.33
	0.2	15.1	6.17	18.0	7.26	17.2	6.85	12.88	3.86	15.5	4.79	14.8	4.50
	0.4	24.4	11.0	29.1	13.1	27.8	12.3	21.1	7.59	25.4	9.29	24.2	8.71
	1	45.9	24.0	54.6	28.0	52.1	26.2	40.3	16.8	48.4	19.9	46.2	18.6
	2	73.8	42.3	87.6	49.4	83.5	46.2	65.6	31.0	78.7	36.9	75.0	34.3
	4	118	73.8	140	86.1	133	80.4	106	56.0	127.3	66.0	121	61.5
	10	218	152	257	176	245	165	200	120	239	140	227	131
2.0	0.1					5.49	1.73						
	0.2			6.35	2.18	8.91	3.34					7.52	1.87
	0.4	5.52	1.88	10.29	4.22	14.4	6.01			8.66	2.34	12.3	3.76
	1	10.4	4.47	19.4	9.08	27.1	12.9	8.74	2.48	16.6	5.94	23.5	9.06
	2	16.8	8.02	31.3	16.4	43.6	22.9	14.3	5.06	27.1	11.3	38.3	16.1
	4	27.0	14.4	50.2	28.9	69.8	40.3	23.2	9.84	44.0	20.4	62.0	29.5
	10	50.3	30.5	93.3	60.3	129	83.2	44.0	21.6	83.1	45.1	117	63.4

C:\Users\sb11\Documents\Papers in progress\Refrigerant + Oil\New paper calc film thickness\Results_Oil_Refrigerant_Mixture-3a.xlsx

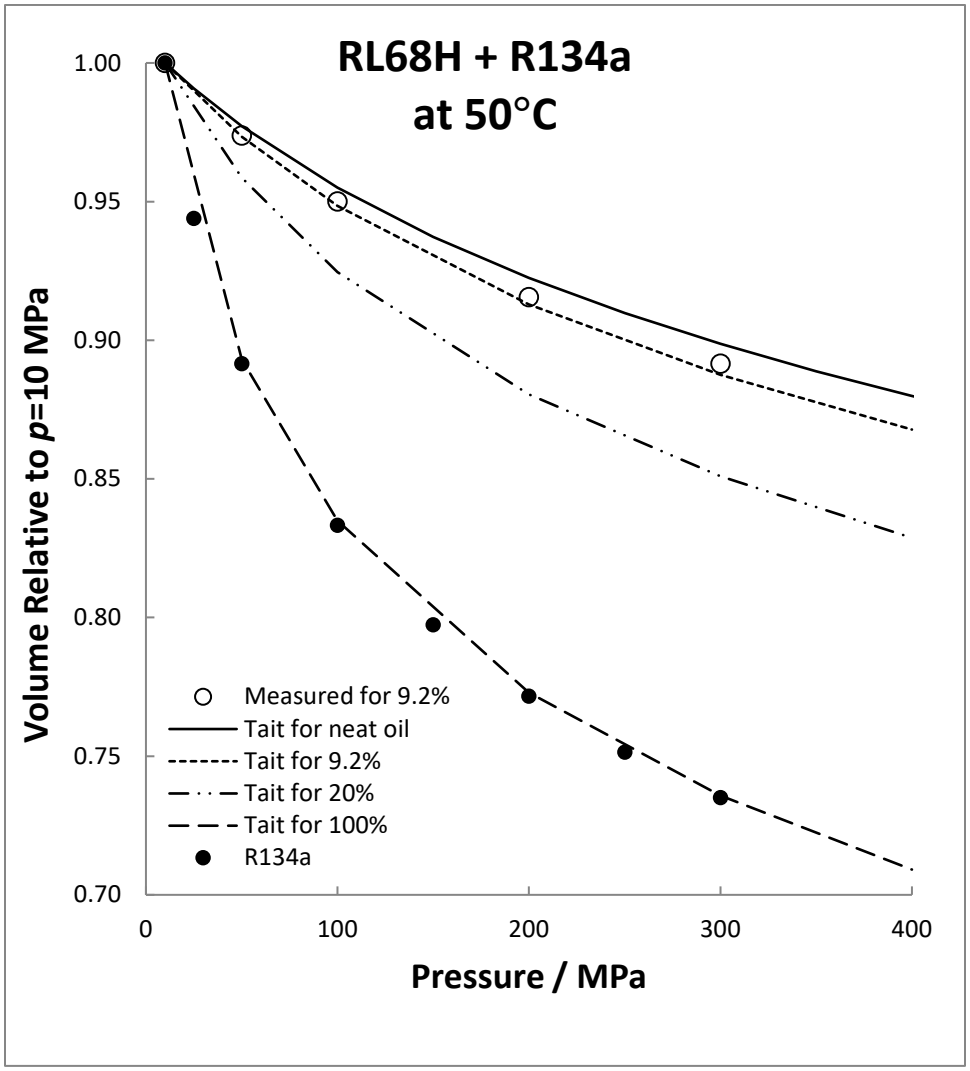

C:\Users\sb11\Documents\Modeling Data\Wassim 2016\Tait for mix.xlsx

Figure 1. Validation of the new EoS at 50°C. R134a from reference [22].

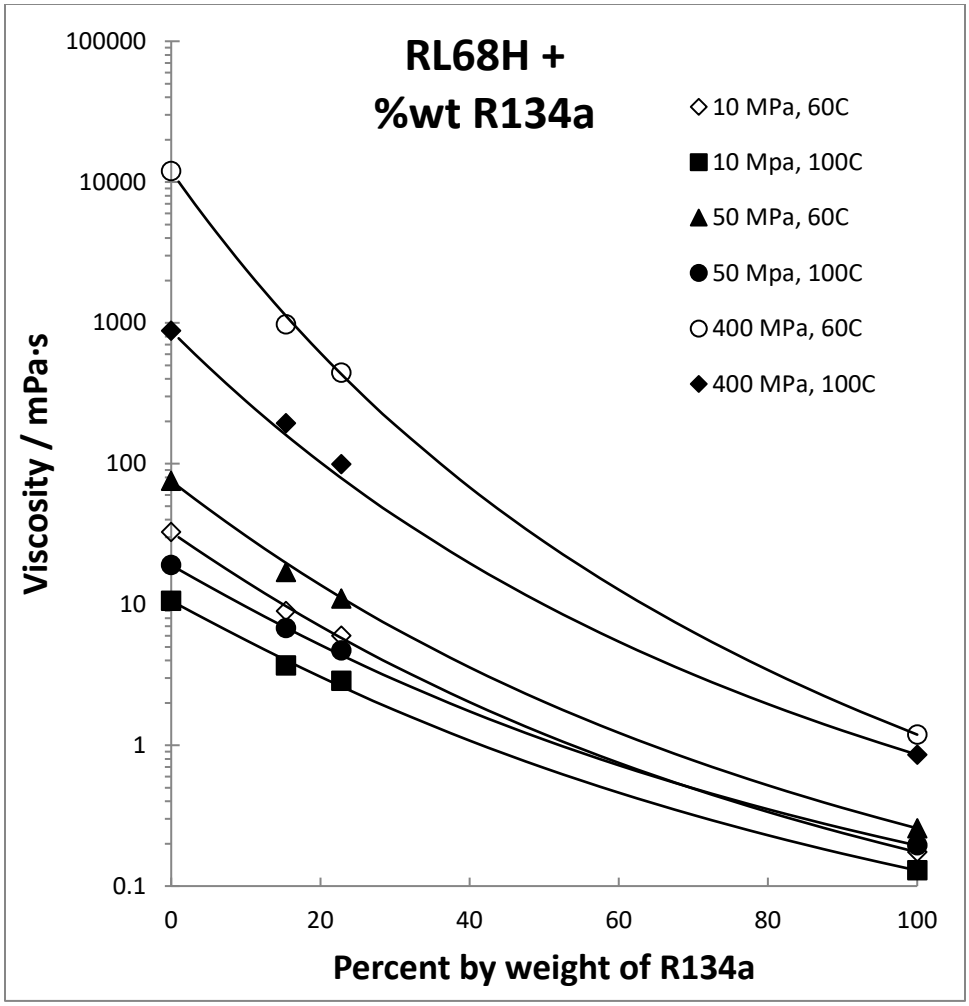

C:\Users\sb11\Documents\Modeling Data\Wassim 2016\Tait for mix.xlsx

Figure 2. Mixing chart for the oil/refrigerant system.

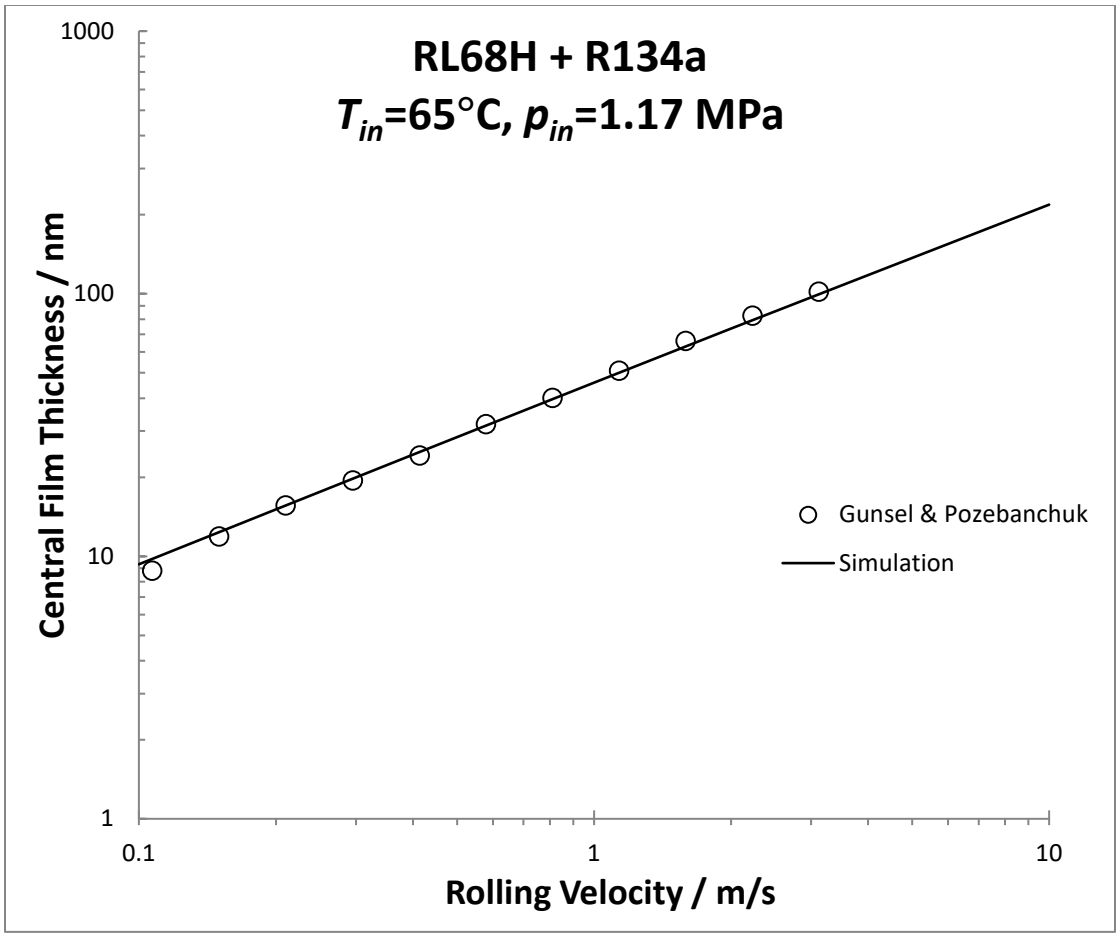

C:\Users\sb11\Documents\Papers in progress\Refrigerant + Oil\New paper calc film thickness\Gunsel validation 2.xlsx

Figure 3. Comparing the present simulation with experiment of Gunsel and Pozebanchuk [28].

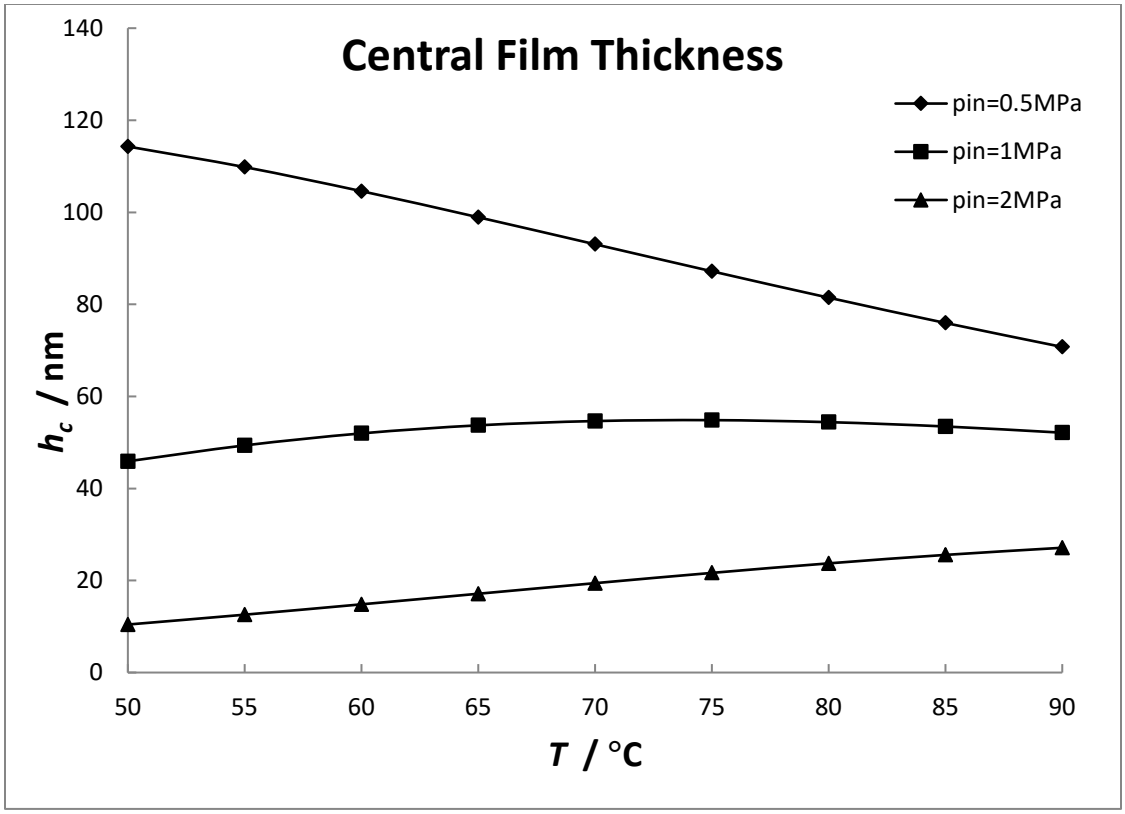

C:\Users\sb11\Documents\Papers in progress\Refrigerant + Oil\New paper calc film thickness\Results_Oil_Refrigerant_Mixture-3a.xlsx

Figure 4. Central film thickness for Hertz pressure of 0.7 GPa and 1 m/s versus inlet temperature for three inlet pressures.

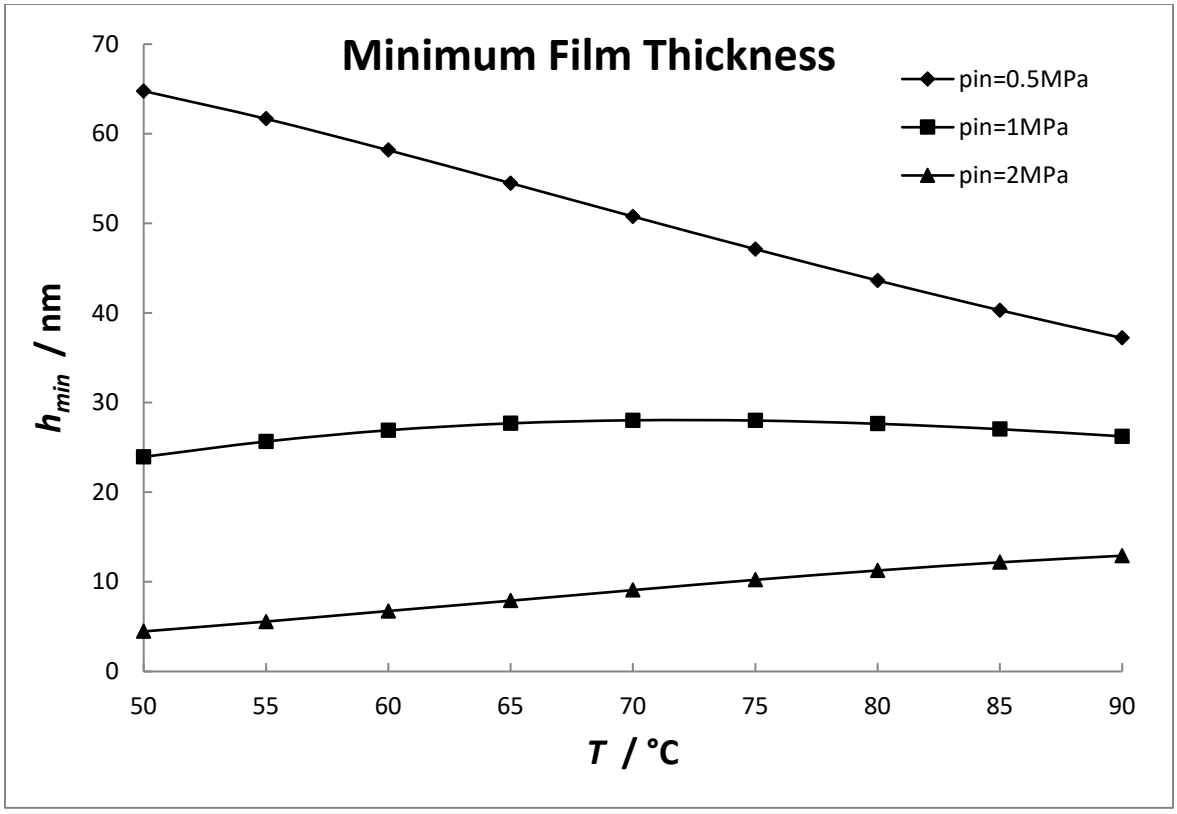

Figure 5. Minimum film thickness for Hertz pressure of 0.7 GPa and 1 m/s versus inlet temperature for three inlet pressures.

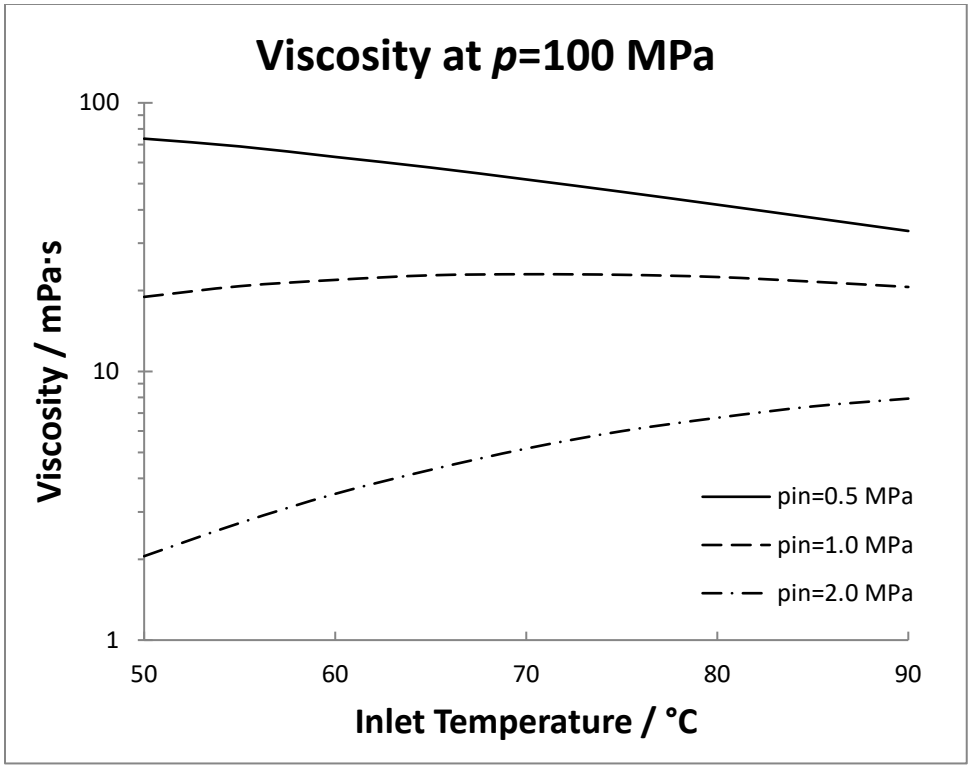

Figure 6. The viscosity at p=100 MPa as a function of inlet temperature for three inlet pressures.

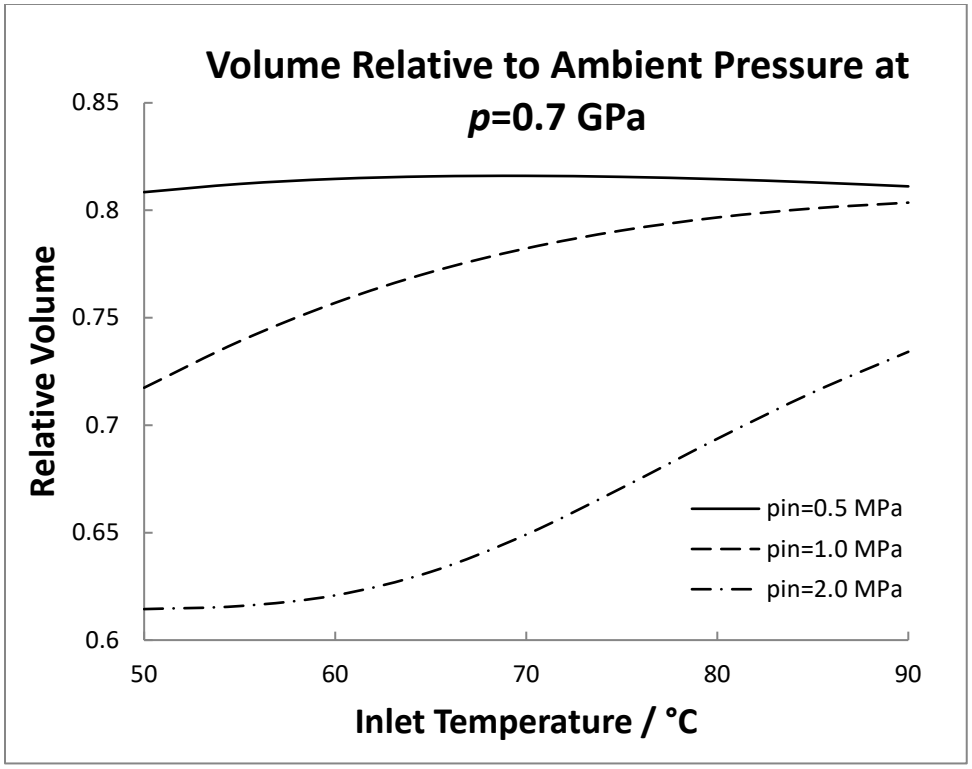

Figure 7. Volume at p=0.7 GPa relative to the volume at ambient pressure as a function of inlet temperature for three inlet pressures.